Electron momentum density of hexagonal zinc studied by Compton scattering

2001 J. Phys.: Condens. Matter 13 11597

(http://iopscience.iop.org/0953-8984/13/50/318)

INSTITUTE OF PHYSICS PUBLISHING JOURNAL OF PHYSICS: CONDENSED MATTER

J. Phys.: Condens. Matter **13** (2001) 11597–11606 PII: S0953-8984(01)18792-8

Electron momentum density of hexagonal zinc studied by Compton scattering

H Reniewicz[1], A Andrejczuk[1,2], L Dobrzyński[1,3,4], E Żukowski[1] and S Kaprzyk[5]

[1] Institute of Experimental Physics, University of Bialystok, ul. Lipowa 41, 15-424 Bialystok, Poland
[2] Institute of Physics, Polish Academy of Sciences, Al. Lotnikow 32/46, 02-668 Warszawa, Poland
[3] Laboratoire de Mineralogie et Cristallographie, Université Pierre et Marie Curie (Paris VI), 4, pl. Jussieu, 75252 Paris, France
[4] The Soltan Institute for Nuclear Studies, 05-400 Otwock-Świerk, Poland
[5] Faculty of Physics and Nuclear Techniques, Academy of Mining and Metallurgy, Al. Mickiewicza 30, 30-059 Kraków, Poland

E-mail: ren@alpha.uwb.edu.pl (H Reniewicz)

Received 7 November 2000, in final form 20 September 2001
Published 30 November 2001
Online at stacks.iop.org/JPhysCM/13/11597

Abstract

We have measured the directional Compton profiles of a single crystal of hexagonal zinc along the [00·1], [10·0], [11·0] and [11·1] directions using high-energy (662 keV) gamma radiation from a ^{137}Cs isotope source. The experimental data have been compared with the corresponding theoretical Korringa–Kohn–Rostoker semi-relativistic calculations. The theory slightly overestimates the electron momentum densities at low momenta regions for all measured profiles. The directional difference profiles, both experimental and theoretical, show very small anisotropy of the electron momentum density in hexagonal zinc, at most half of that presented in the literature for cubic systems.

1. Introduction

Compton scattering is a well-established method for investigating electronic structures in condensed matter physics [1–3]. The spectrum of inelastically scattered monoenergetic photons from electrons in a target is related through the Doppler effect with the electron momentum–density distribution. The one-dimensional projection, $J(p_z)$, of the electron momentum–density distribution, $n(\boldsymbol{p})$, along a given direction (usually chosen to be the z-axis) is called the Compton profile (CP)

$$J(p_z) = \iint n(\boldsymbol{p})\, \mathrm{d}p_x\, \mathrm{d}p_y \tag{1}$$

which is naturally normalized to the number of electrons per formula unit. Subtraction of the profiles measured at two specific crystallographic directions removes the isotropic core–electron contributions and forms the so-called difference profile which shows the anisotropy of the electron momentum–density in the material under study. When the absolute values of the CPs can bear some systematical error, this anisotropy still provides valuable information on the behaviour of the outer electrons responsible for creation of solids and their properties.

Zinc is a so-called 'marginal' material, because it is the last material in the 3d row in the periodic table of elements. It is known that the calculated d-bands for such metals (e.g. Cu, Zn) are not well described, particularly because of the self-interaction correction, which has to be introduced properly to the local density approximation (LDA) [4]. In spite of theoretical efforts, the calculated position of the d-band with respect to the Fermi energy, and the width of the d-band, still do not agree very well with the angle-resolved photoemission studies by Himpsel *et al* [5]. According to these authors, Zn is an almost ideal material to study the degree of itinerancy of the 3d-electrons, and to understand it requires theory which goes beyond the LDA. Recently, the study of zinc has been given additional interest because of the predicted series of electronic topological transitions under pressure [6]. In [6] the authors followed the observed changes in the lattice properties of Zn and Cd under pressure [7,8]. It was found that these changes were again not too well described by theory, which requires a rather detailed knowledge of the electronic structure of zinc. This has motivated us to study the CPs in zinc and other hexagonal close-packed (hcp) metals, both experimentally and theoretically.

While the CPs of polycrystalline samples of zinc have been studied using 59.5 keV radiation from a ^{241}Am source [9, 10] and 662 keV radiation from a ^{137}Cs source [11], no experimental Compton studies performed on single-crystal samples have been published. The electron momentum–density distribution in Zn has been studied using the positron annihilation method (see, for example, [12–14]), but it is known that this method has certain drawbacks especially where the studies of electron–electron correlations are concerned. This present study has been undertaken to investigate the anisotropy of the electron momentum–density distribution for zinc and to test the feasibility of Korringa–Kohn–Rostoker (KKR) technique in calculations of CPs for hexagonal-structured materials. This last problem is by no means trivial in view of important differences found between KKR calculations and the experiment for another hexagonal metal, namely beryllium [15].

Zinc crystallizes in A3 hcp structure with the lattice parameters $a = 0.2665$ nm and $c = 0.4947$ nm and with two atoms in the unit cell [16]. The lower (as compared with simple cubic systems) symmetry induces difficulties in theoretical calculations. The theoretical calculations of CPs published for non-primitive crystals, the renormalized free atom (RFA) model and the orthonormalized linear combination of atomic orbitals (LCAO) [9, 17] show significant discrepancies between experiment and theory. As we shall see, the present calculations performed within the KKR scheme describe the experimental results much better. This does not mean that the electronic structure of zinc is now fully understood.

2. Experimental details

Four directions have been chosen for the investigation: [00·1] (direction Γ–A in first Brillouin zone), [10·0] (direction Γ–M), [11·0] (direction Γ–K) and [11·1]. The adopted system of the indexing of directions and planes in the hexagonal structure is shown in table 1 together with the sample parameters. The experiment was performed at the Institute of Experimental Physics, University of Bialystok, Poland, on the high-energy Compton spectrometer. A ^{137}Cs source emits photons of energy, 661.65 keV, which are scattered on electrons in the sample through the angle $\theta = 165^{\circ}$ and registered by the high-purity germanium (HPGe) detector.

Table 1. Details of the experiment and characteristics of the hexagonal zinc samples.

Crystallographic directions (in reciprocal space) along the normal to the surface of the sample	[00·1]	[10·0]	[11·0]	[11·1]
Equivalent special directions in the first Brillouin zone	Γ–A	Γ–M	Γ–K	[a]
Miller indices of corresponding planes (in real space) perpendicular to given directions and parallel to the surface of the sample	(0001)	$(10\bar{1}0)$	$(11\bar{2}0)$	$(11\bar{2}1)$
Thickness of the sample (mm)	1.3	1.0	1.2	0.8
Measuring time (h)	340	630	370	400
Counts under Compton profile in the range from −10 au to +10 au	3.8×10^7	4.7×10^7	3.4×10^7	3.7×10^7
Counts at the maximum of Compton peak. Channel width of the multichannel analyser of the Compton spectrum is equal to 61 eV	3.4×10^5	3.9×10^5	2.8×10^5	3.1×10^5
Level of multiple scattering (multiple/single) (%)	11.3	10.1	11.6	8.1
Signal-to-background ratio	300:1			
Number of electrons in momentum range 0–10 au	13.864			

[a] Direction [11·1] in reciprocal space is inclined from direction Γ–H in the first Brillouin zone (also indicated as [11·1]) by about 7°.

The source-to-sample and sample-to-detector distances are 422 and 666 mm, respectively. The total momentum resolution of the measurement is 0.42 au (1 au of momentum = 1.9929×10^{-24} kg m s^{-1}). The spectrometer itself and the experimental data handling procedures have been described elsewhere [18, 19]. The zinc crystals were grown by the Bridgeman method at the Institute of Nuclear Research in Świerk, Poland. The samples have been cut from the ingot, etched and checked for orientation using the x-ray Laue technique. The size of the sample face used in the experiment was typically 15×15 mm^2. The thickness of the samples and parameters of the measurements are given in table 1. Another set of measurements, with comparable statistics, was carried out with samples of rectangular shape and with the size of the sample face being 15×50 mm^2. The stability of the electronics and energy calibration have been checked during the measurements and no more than 0.5 channel per month drift was observed (channel width is equal to 61 eV). Unfortunately, during the measurements with the square samples the detector failed and it had to be replaced by a new one with nominally the same characteristics. Nevertheless, it was found that the two series of measurements gave much the same difference profiles.

The total CPs, $J(p_z)$, were extracted from the experimental spectrum after a number of energy-dependent corrections were included in the standard procedure (see, for example, [18, 19]). The experimental CPs have been normalized in the range from 0 to +10 au to 13.864 electrons, i.e. to the data obtained from the theoretical free-atom CP of zinc [20]. The effect of multiple scattering of photons in the sample, which builds an unwanted background in the measured spectrum, was simulated by the Monte Carlo method [21] and subtracted from the final CPs. The fraction of multiple to single scattering events was found to amount to 11% in the range 0–10 au. As was mentioned in [22], in the experiments with high-energy photons

and a sample of high Z, some sort of additional background appears. The source of this background is not yet known. We commonly apply additional correction for this effect by subtracting a constant background from the profile. The level of this background is fitted to give the best agreement between the experiment and theory in the range 5–10 au, where the known core profile dominates and the contribution from the valence electrons is negligible. In the present experiment, the value of the additional background has been estimated to be 1.5% of the area under the total CP. The systematic effect of the additional background is automatically cancelled when the experimental difference profiles (anisotropies) are calculated.

Our Compton spectrometer is based on the gamma source, which delivers a large irradiation area at the sample position (the diameter of the full beam is 15 mm), so a good account of the full geometry of the experiment is not trivial. In particular, the Monte Carlo procedure used to simulate multiple scattering, which must be finally subtracted from the measured spectra, only provides data of limited accuracy. As was mentioned, in order to reach the agreement of the absolute CP with that calculated for free atoms at high momenta, an additional constant background has to be subtracted from the data. Although in many cases this additional correction changes the values of the CP at high momenta by less than 0.02 electrons per au, the normalization condition means that the changes at high momenta result in the opposite changes at the origin of the profile. Because of the problems with the detector, in the following we discuss the CPs measured mainly on the rectangular-shaped samples. An exception to this is the [00·1] direction, which was measured on the square sample, being the only sample available. A direct comparison of the results obtained on rectangular and square samples is not straightforward because the different geometrical conditions of measurements result in slightly different resolutions. Nevertheless we should stress that the data obtained on the square samples are not in conflict with the data on rectangular samples.

3. Theory

The first KKR calculations of momentum–density distribution in hcp structure were published for beryllium [15, 23] The present electronic band and momentum density computations of hexagonal Zn (carried out for the first time for a transition metal) are based on the KKR Green function method, utilizing the muffin-tin approximation to the crystal potential [24–26]. All electrons were included and the von Barth–Hedin [27] LDA to the exchange–correlation potential was used. The band-structure problem was solved to a high degree of self-consistency (energy bands, Fermi energy, and potentials converged to better than 1 meV) for the Zn hexagonal lattice (lattice constants: $a = 5.0284$ au, $c = 9.3578$ au) using $l_{\max} = 3$ (maximum angular momentum cut-off). In order to find the CPs, the momentum–density $n(\boldsymbol{p})$ of equation (1) was calculated (see [28] for details) on a mesh containing $24 \times 3153 \times 2799\boldsymbol{p}$ points; here 24 denotes the number of symmetry operations of the hexagonal point group, 3153 is the number of $\boldsymbol{k}$ points non-uniformly distributed (with 2417 points sitting on the Fermi surface sheets) in the irreducible 1/24th of the Brillouin zone, and 2799 is the number of $\boldsymbol{p}$ points obtained from each $\boldsymbol{k}$ point by adding reciprocal lattice vectors. The two-dimensional integrations involved in the evaluation of CPs were carried out by using the tetrahedral method of Lehmann and Taut [29]. This approach can be very efficient since the form (3.20) from [29] is especially amenable to developing highly vectorized computer codes. The final CPs were computed along the [00·1], [10·0], [11·0] and [11·1] directions on a 201-point uniformly spaced mesh in $\boldsymbol{q}$ (momentum transfer) over the range 0–15 au. Based on a variety of computations in which different meshes were used, we estimate that our calculated CPs are accurate to about five parts in 10^4. The Lam–Platzman correction was calculated in the final stage in a standard way using all the electrons as required by the LDA method.

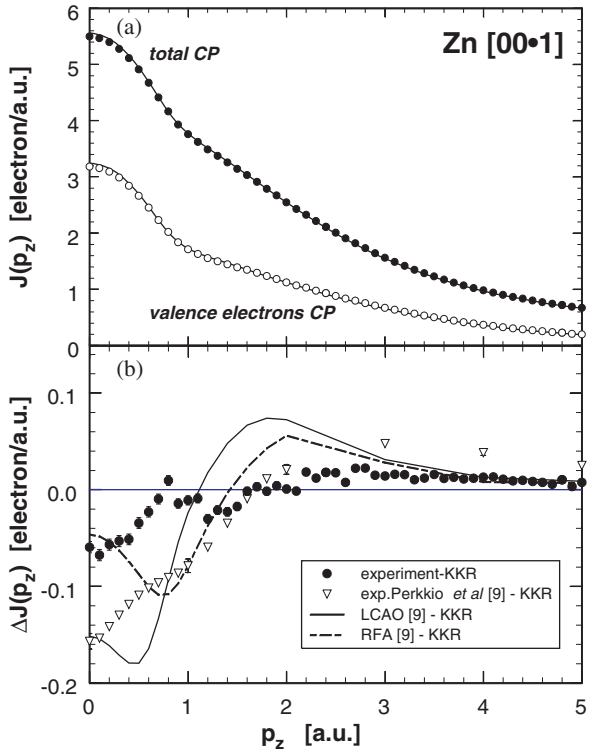

Figure 1. The absolute CP of hexagonal Zn for the [00·1] direction. The upper panel (a) presents the total and valence electron profiles. The experimental data are shown by the solid circles (the total profile) and the open circles (the valence profile for $3d^{10}4s^2$ electrons) while the theoretical KKR data are plotted by the solid curves. The experimental valence CP was calculated by extracting the theoretical KKR core profile from the total experimental data. The experimental statistical errors are much smaller than the size of the symbols. The lower panel (b) shows the differences between the profiles indicated in the legend and the recent KKR data, directionally averaged. The difference observed in the present experiment is represented by the solid circles. The difference for an earlier experiment performed on polycrystalline zinc [9] with the use of a ^{241}Am source is shown by open triangles. A proper amount of $1s^2$ profile has been added to the experimental profile at momentum $p_z > 2.2$ au (see the text for an explanation). The differences for LCAO and RFA data [9] are plotted by the solid and dashed curves, respectively. All theoretical CPs have been normalized to the same number of electrons and convoluted with a Gaussian of FWHM = 0.42 au to mimic the experimental resolution. In the case of ^{241}Am experiments the KKR theory before subtraction was convoluted with the RIF function taken from [9].

4. Discussion of the results

As an example, the absolute CP of Zn is shown in figure 1 for the [00·1] direction, i.e. along the *c*-axis. Figure 1(a) presents the total (solid circles) and the valence electron (open circles) experimental profiles. The solid curves in figure 1(a) represent the theoretical KKR data. The experimental statistical error bars are smaller than the size of the points. The experimental valence CPs ($3d^{10}4s^2$ electrons) were calculated by extracting the theoretical KKR core profiles from the experimental CPs. Small differences (smaller than about 0.06 electrons per au) between experiment and theory are seen, especially in the momentum region $p_z < 1$ au which also covers the range of the valence $4s^2$ electron profile. The valence profile of $3d^{10}$ electrons extends far beyond the displayed momentum region of 5 au (in practice, this profile falls below 0.01 electrons per au at $p_z > 10$ au only).

The lower panel, figure 1(b), shows the difference between present experiment and theory, represented by solid circles. The KKR theory seems to fail in reproducing the experiment in the already-mentioned momentum region below 1 au. However, the surplus of theoretical values above experimental values at the origin of the CPs is commonly recognized and accepted [30–35]. We also present in figure 1(b) the differences between the KKR calculations (directionally averaged) and the Compton data for polycrystalline zinc measured by Perkkio *et al* [9] with the use of a ^{241}Am source (open triangles). The energy of photons from the ^{241}Am source (60 keV) is too low for Compton scattering on K-shell electrons with $p_z > 2.2$ au, so their contribution to the profile could not be observed in the original experiments. Thus, in order to compare this experiment with our data, a proper amount of $1s^2$ electron profile had to be added to the difference profile. We also made a convolution of the KKR data using the residual instrument function (RIF) function from the experiment by Perkkio *et al* [9]. Perkkio *et al* [9] have also presented theoretical LCAO and RFA Compton profiles. In order to compare these with our KKR results and—indirectly—with our experiment, all calculated profiles were convoluted with the Gaussian shape resolution function of 0.42 au. The differences LCAO–KKR and RFA–KKR in the theoretical results are plotted by the solid and dashed curves, respectively. It is clearly seen that both LCAO and RFA calculations completely fail in describing the measured profiles at momenta below 3 au. As will be shown later, the profiles measured along different directions parallel to the hexagonal basal plane or directions out of both *a* and *c* planes differ from the presented [00·1] profile by no more than by 0.02 electrons per au. Therefore, the conclusion on the failure of the calculations given in [9] is generally valid.

The absolute profiles, both experimental and theoretical, have been used to form the directional difference profiles indicating the anisotropy of the electron momentum–density distribution in hexagonal zinc. The measured and calculated anisotropies are shown in figure 2 for six pairs of directions indicated on the graphs. Figures 2(a) and (b) present the differences between orthogonal, basal and [00·1] directions. Figure 2(d) characterizes the anisotropy in the basal plane whereas three panels, figures 2(c), (e) and (f), present the differences between the out-of-basal plane [11·1] direction, and [00·1] and basal directions. Inspection of figure 2 shows that the experimental anisotropies are in qualitative agreement with KKR band theory, i.e. indications of the periodicity of the oscillations are correct, and the amplitudes of theoretical anisotropies are on the same level as the experimental anisotropies. The only apparent differences are seen in figures 2(b) and (e), in which peaks expected at 0 and 2 au, respectively, are definitely not seen in the experiment. The electron momentum–density in zinc shows surprisingly small anisotropy, 0.02 electrons per au at most. An anisotropy much lower than that known for cubic systems (see, for example, [18, 30–32, 36]) can probably be expected, based on the purely geometrical properties of the lattice. Similarly small anisotropy has been observed recently in rhombohedral bismuth [37]. However, it is also well known that observed amplitudes of the oscillations in cubic systems (in which anisotropy itself reaches 0.05–0.1 electron per au) are as a rule two times lower than theory indicates. This may be contrasted with observations for Zn where the theoretical amplitude of oscillation seems to agree with experiment. Perhaps the relative agreement of the experimental and theoretical amplitudes of oscillations is due to some cancellation effects of the relativistic and correlation effects, as was the case in otherwise cubic Ag [18]. Beyond doubt, however, much better experimental accuracy is required for clarification of this point. We are also aware that the relativistic effect in Zn ($Z = 30$) might not be so evident as in Ag ($Z = 47$).

It could be expected intuitively that the largest anisotropy in the electron momentum–density distribution should first of all be observed between the *c*-axis and any direction in the basal plane. This is actually true for the [11·0]–[00·1] difference (figure 2(b)).

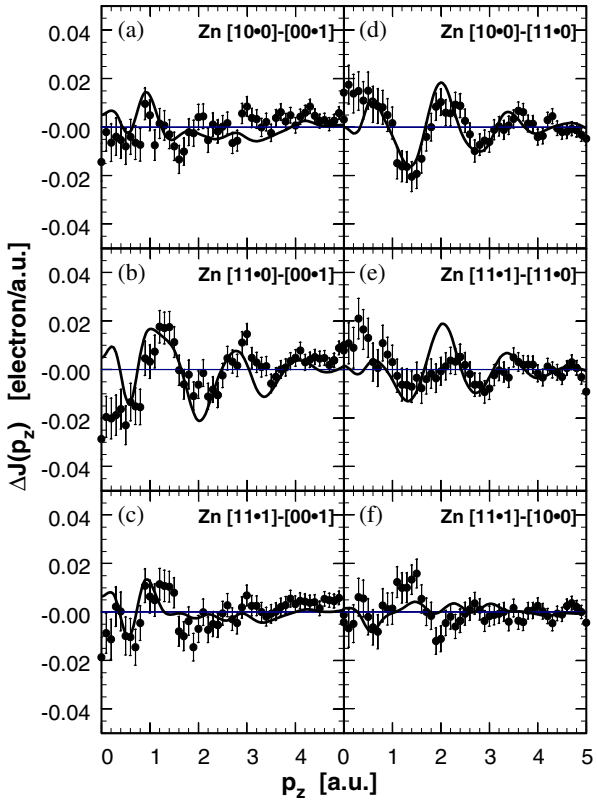

Figure 2. The measured and calculated anisotropies of the CPs in a single crystal of Zn for the six difference profiles indicated in the panels. All theoretical CPs have been convoluted with a Gaussian of FWHM = 0.42 au to mimic the experimental resolution (see the text for details and discussion).

For comparison, the experimental anisotropy [10·0]–[00·1] (figure 2(a)) is statistically insignificant. Indeed, atomic distributions along these two directions are quite similar, so one cannot also expect large anisotropy in the momentum space. For the largest anisotropies, figures 2(b) and (d), an apparent disagreement between theory and experiment is visible at low electron momenta (say, below 0.5 au). The differences reach the level of 0.02 electrons per au, which is much lower (due to subtraction) than in the case of absolute profiles (0.06 electrons per au shown as an example in figure 1(b)). One may compare the presented CPs of hexagonal zinc with the CPs of hexagonal beryllium. The latter were intensively studied in Compton experiments with moderate resolution (0.4 au, [38]) and high resolution (0.15 au, [15,23,39]). The experimental CP directional anisotropies have been compared with pseudopotential calculations used within the local density-functional approach [40] where reasonable agreement was found. A similar agreement of the experiment and KKR theory has been reported in [15] and [23]. Comparing the CP anisotropies in Be and Zn one can notice that the oscillations in Be are already decayed below about 1.5 au, whereas they are seen in zinc beyond 5 au. The amplitude of the oscillations in Be (see, for example, figure 5 in [15]) is also essentially larger than in Zn. KKR theory explains this quite well while it overestimates the oscillations in Be. This overestimation is usually interpreted as due to the incomplete treatment of the electron correlations. We also note that the experiment [15] has revealed

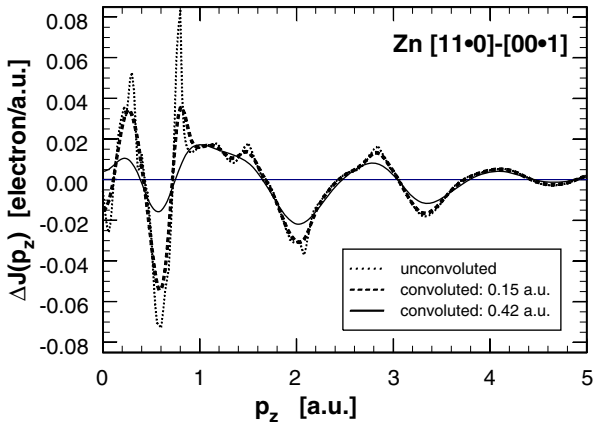

Figure 3. The [11·0]–[00·1] anisotropy of the theoretical KKR CP in Zn shown for different resolutions. The unconvoluted theoretical data are plotted as the dotted curve. The dashed and solid curves show the same anisotropy for constituent profiles convoluted with a Gaussian of FWHM = 0.15 au and 0.42 au, respectively. The latter anisotropy is also presented in figure 2(b) together with the experimental data.

important differences between calculated and experimental fermiological features in CPs. The typical features of this kind expected for zinc are displayed in figure 3. Very abrupt changes of anisotropy are expected in the region 0–1 au. The singularities are quickly washed out with the deterioration of the momentum resolution, and certainly cannot be observed with our modest resolution. Nevertheless we should note that similar singularities expected for beryllium have never been experimentally detected. The precision and momentum resolution of our experiment does not allow us to analyse this kind of problem in detail. We should like to stress that the differences between experiment and theory seen in figure 2(b) for momenta below 0.5 au, and the lack of the expected peak in figure 2(e) at $p_z = 2$ au, might already suggest that the KKR calculations for hexagonal metals should be improved. Huotari *et al* [41], analysing similar discrepancies between the experimental and theoretical CPs of Be, have suggested that an isotropic Lam–Platzman correction is not adequate and a better treatment of the correlation effects in inhomogeneous electron gas is needed. Figure 4 shows the appropriate difference CPs (i.e. the discrepancies between the experiment and Lam–Platzman corrected theory in relation to the Lam–Platzman correction itself) for Zn crystals in our data. Indeed, the observed differences are almost twice the height of the Lam–Platzman correction at momenta $p_z < 0.6$ au. However, the differences are not so strongly direction-dependent as was observed in Be [41]. We note, however, that particularly large differences are observed at $p_z = 0$ au.

5. Summary and conclusions

The [00·1], [10·0], [11·0] and [11·1] directional Compton profiles of hexagonal zinc have been measured for the first time with the use of a high-energy ^{137}Cs gamma ray source. Also, the KKR calculations have been applied for the first time to hcp Zn. In spite of the substantial improvement of the KKR approach over earlier approaches, i.e. RFA and LCAO calculations, the theory predicts a CP which is too high at low momenta ($p_z < 1$ au) with values which are correspondingly too low at higher momenta. The amplitude of theoretical anisotropy of the CPs of Zn agrees rather well with the measured data and the main differences are seen at the origin of the CPs only. The anisotropies in the hexagonal structure of Zn are at most half of that

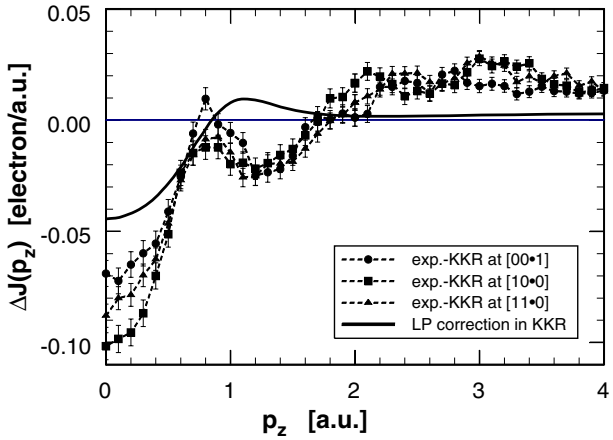

Figure 4. Difference between the experimental and theoretical Lam–Platzman corrected KKR CPs along the [00·1], [10·0] and [11·0] directions shown by solid circles, triangles and rectangles, respectively. The Lam–Platzman correction itself is represented by the solid curve. The thin dashed curves are drawn to guide the eyes. Note that the area under the difference profiles are normalized to zero electrons in the range 0–10 au.

measured for high symmetry cubic systems. However, the anisotropy of the CP of Zn extends to much larger electron momenta than in the other well-known hcp metal, beryllium. We have found definite differences between KKR calculations and the experimental data, which call for improved calculations, especially at low momenta where we observe that the Lam–Platzman correction for electron correlation effects might be reproduced inadequately. Doubtless an experiment carried out with better resolution and statistics would allow us to obtain much better insight into the fermiological aspects of Zn and into the problem of electron correlations in Zn.

Acknowledgments

This work has been sponsored by the Committee for Scientific Research (KBN) in Poland through grant no 2 P03B 012 18. We are grateful to Mr J Waliszewski for valuable comments. Dr S Chabik from the Institute of Physics, University of Opole, is gratefully acknowledged for providing us with the crystal of zinc.

References

[1] Cooper M J 1985 *Rep. Prog. Phys.* **48** 415
[2] Schülke W 1989 *Nucl. Instrum. Methods* A **280** 382
[3] Dobrzyński L 1993 *Z. Naturf.* A **48** 266
[4] Norman M R 1984 *Phys. Rev.* B **29** 2956
[5] Himpsel F J, Eastman D E, Koch E E and Williams A R 1980 *Phys. Rev.* B **22** 4604
[6] Novikov D L, Katsnelson M I, Trefilov A V, Freeman A J, Christensen N E, Svane A and Rodriguez C O 1999 *Phys. Rev.* B **59** 4557
[7] Takemura K 1995 *Phys. Rev. Lett.* **75** 1807
Takemura K 1997 *Phys. Rev.* B **56** 5170
[8] Potzel W, Steiner M, Karzel H, Schiessl W, Köfferlein M, Kalvius G M and Blaha P 1995 *Phys. Rev. Lett.* **74** 1139
[9] Perkkio S, Sharma B K, Manninen S, Paakkari T and Ahuja B L 1991 *Phys. Status Solidi* b **168** 657
[10] Pal D and Padhi H C 1991 *Phys. Status Solidi* b **163** K129

[11] Chu-Nan Chen 1989 *Chin. J. Phys.* **27** 461
[12] Chabik S 1974 *PhD Thesis* University of Wroclaw, Wroclaw
[13] Rozenfeld B and Chabik S 1977 *Appl. Phys.* **13** 81
[14] Daniuk S, Kontrym-Sznajd G, Rubaszek A, Stachowiak H, Wayers J, Walters P A and West R N 1987 *J. Phys. F: Met. Phys.* **17** 1365
[15] Hämäläinen K, Manninen S, Kao C-C, Caliebe W, Hastings J B, Bansil A, Kaprzyk S and Platzman P M 1996 *Phys. Rev.* B **54** 5453
[16] Wyckoff R W G 1963 *Crystal Structures* (New York: Wiley)
[17] Aikala O 1975 *Phil. Mag.* **31** 935
Aikala O 1967 *Phil. Mag.* **33** 603
[18] Andrejczuk A, Dobrzyński L, Kwiatkowska J, Maniawski F, Kaprzyk S, Bansil A, Żukowski E and Cooper M J 1993 *Phys. Rev.* B **48** 15 552
[19] Andrejczuk A, Żukowski E and Dobrzyński L, Cooper M J 1993 *Nucl. Instrum. Methods* A **337** 133
[20] Biggs J, Mendelsohn L B and Mann J B 1975 *At. Data Nucl. Data Tables* **16** 201
[21] Felsteiner J, Pattison P and Cooper M J 1974 *Phil. Mag.* **30** 537
[22] Bansil A, Kaprzyk S, Andrejczuk A, Dobrzyński L, Kwiatkowska J, Maniawski F and Żukowski E 1998 *Phys. Rev.* B **57** 314
[23] Itou M, Sakurai Y, Ohata T, Bansil A, Kaprzyk S, Tanaka Y, Kawata H and Shiotani N 1998 *J. Phys. Chem. Solidi* **59** 99
[24] Bansil A 1987 *Electronic Band Structure and its Applications (Lecture Notes in Physics vol 283)* ed M Yussouff (Heidelberg: Springer) p 273
Bansil A, Kaprzyk S and Tobola J 1992 *Applications of Multiple Scattering Theory to Materials Science (MRS Symp. Proc. vol 253)* ed W H Butler *et al* (Pittsburg, PA: Materials Research Society) p 505
Bansil A, Rao R S, Mijnarends P E and Schwartz L 1981 *Phys. Rev.* B **23** 3608
[25] Kaprzyk S and Bansil A 1990 *Phys. Rev.* B **42** 7358
[26] Bansil A and Kaprzyk S 1991 *Phys. Rev.* B **43** 10 335
[27] Von Barth U and Hedin L 1972 *J. Phys. C: Solid State Phys.* **5** 1629
[28] Kaprzyk S 1997 *Acta Phys. Pol.* A **91** 135
[29] Lehmann G and Taut M 1972 *Phys. Status Solidi* b **54** 469
[30] Rollason A J, Holt R S and Cooper M J 1983 *Phil. Mag.* B **47** 51
[31] Chu-Nan Chang, Mei-Ling Dy and Huey-Fen Liu 1995 *Chin. J. Phys.* **33** 159
[32] Cardwell D A, Cooper M J and Wakoh S 1989 *J. Phys.: Condens. Matter* **1** 541
[33] Kothari R K, Joshi K B, Sharma M D, Ahuja B L and Sharma B K 1995 *Phys. Status Solidi* b **190** 475
[34] Schülke W, Stutz G, Wohlert F and Kaprolat A 1996 *Phys. Rev.* B **54** 4381
[35] Pandya R K, Joshi K B, Jain R, Ahuja B L and Sharma B K 1997 *Phys. Status Solidi* b **200** 137
[36] Żukowski E *et al* 1997 *J. Phys.: Condens. Matter* **9** 10 993
[37] Andrejczuk A, Reniewicz H, Dobrzyński L, Żukowski E and Kaprzyk S 2000 *Phys. Status Solidi* b **217** 903
[38] Hansen N K, Pattison P and Schneider J R 1979 *Z. Phys.* B **35** 215
[39] Loupias G, Petiau J, Issolah A and Schneider M 1980 *Phys. Status Solidi* b **102** 79
[40] Chou M Y, Lam P K and Cohen M L 1983 *Phys. Rev.* B **28** 1696
[41] Huotari S, Hämäläinen K, Manninen S, Kaprzyk S, Bansil A, Caliebe W, Buslaps T, Honkimäki V and Suortti P 2000 *Phys. Rev.* B **62** 7956